Egyptian Geophysical Society
EGS Journal, Vol. 8, No. 1, 159-180 (2010)

GEOLOGICAL AND GEOPHYSICAL INVESTIGATIONS OF THE BRECCIA, SOUTH GABAL MONQUL, NORTHERN EASTERN DESERT, EGYPT

I.M. Gaafar, Kh.G. Ali and T.M. Ibrahim

Nuclear Materials Authority, P. O. Box 530, Maadi, Cairo, Egypt

التحقيقات الجيولوجية والجيوفيزيقية لبريشيا جنوب جبل منقول، شمال الصحراء الشرقية، مصر

الخلاصة: تهتم هذه الدراسة بتمعدنات النحاس والباريوم والذهب في جنوب جبل منقول، شمال الصحراء الشرقية. حيث تنتشر هذه التمعدنات في أجسام البريشيا المتواجدة خلال نطاقات عالية التغاير على حدود الاتصال بين الجرانيت البيوتايتى الخشن الحبيبات والمتداخلات الجرانيتية ذو الاثنين ميكا المتوسط الحبيبات. تتركز هيئات البريشيا فى نطاقات الصدوع المتجهة شرق شمال شرق – غرب جنوب غرب وشمال – جنوب، حيث تصعد السوائل الحرارية المائية والمعدنية مرسبة التمعدنات. يتم العثور على تمعدنات من النحاس، الباريوم والذهب مصاحبة لعمليات البريشيا المكثفة المصاحبة لتواجد هالات من التغاير واسعة المدى.

استطاعت القياسات الإشعاعية الطيفية أن تفصل تماما بين نوعى الجرانيت وكذلك تميز منطقة التغاير الشديد والحاوية للمواد المعدنية. وقد اقترح أن يكون مصدر هذه البريشيا المتمعدنة هو المحاليل الحرارية الحاملة للسوائل المعدنية والمرتبطة بتداخلات الجرانيت ذو الاثنين الميكا. وقد إشتمل العمل الجيوفيزيائى على تطبيق المسح الكهرومغناطيسي ذو التردد المنخفض جدا (VLF-EM) والمسح المغناطيسي. وقد استخدمت هذه الطرق في تحقيق البصمة الجيولوجية والجيوفيزيائية لهذه البريشيا والجرانيت المستضيف. كشفت دراسة التردد المنخفض جدا أن التمعدنات تحت السطحية تتواجد في شكل هيئات ممدوده متطابقة مع السمات التركيبية على السطح. وقد أوضحت الخريطة الكنتورية الناتجة بعد معالجة بيانات الترددات المنخفضة جدا وجود شاذات توصيل عالية. وتختلف قيم التوصيل الخاصة بالبريشيا لكمية ونوعية المتداخلات التى تمتلئ بها. هذا التوصيل القوى والذى ينفصل إلى أجزاء عالية المدى، يقترح أهمية الموقع للاستكشاف. حيث تظهر خريطة الشدة المغناطيسية الأرضية ارتباط نطاق التمعدنات بمنطقة منقول بشاذات عالية ومتطاولة. ويرجع بروز هذا الشذوذ نتيجة للمفارقة الكبيرة فى القابلية المغناطيسية العالية لتمعدنات منطقة منقول مقارنة بالجرانيت المحيط. يثبت تفسير كلا من التردد المنخفض جدا والمغناطيسي أن الاتجاهات التكتونية شرق شمال شرق –غرب جنوب غرب وشمال جنوب ممتدة على أعماق مختلفة ومتطابقة مع السطح.

ABSTRACT: *This study is concerned with Cu, Ba and Au mineralizations in south Gabal Manqul, Northern Eastern Desert. These mineralizations are disseminated in breccia bodies through highly altered contact zone between coarse-grained biotite granite and medium two mica granitic intrusion. These breccia bodies tend to follow the ENE-WSW and N-S faults, where the hydrothermal mineralized fluids passed and the mineralizations were deposited. Extensive alteration haloes have been found where copper, barium and gold mineralization are restricted and exceed with intensive brecciation occurs.*

The spectrometric measurements exactly separate between the two granite types and well discriminate the highly altered and mineralized zone. A hydrothermal origin has been proposed for these mineralized breccias where a high potential mineralized fluid associated the two mica granitic intrusion.

The applied geophysical work includes very low frequency electromagnetic (VLF-EM) and magnetic survey. These methods were used to investigate the geological and geophysical signature of these breccias and their hosted granite. The VLF study revealed that the subsurface mineralization is in the form of elongated bodies concordant with its structural features at the surface. The filtered VLF-EM contour map shows positive conductive anomalies. The breccias have gradational values of conductivity according to the degree of brecciation and the amount of quartz interfragmental filling. This strong conductivity was separated into parts of high amplitudes, resulting in an obvious exploration target.

The ground total magnetic-intensity map shows a relatively elongated anomaly for the Monqul mineralized zone. The prominence of the anomaly can be attributed to the strong contrast between the magnetic susceptibilities of Monqul mineralized zones and the surrounding granites. Both VLF and magnetic interpretation prove the extension of the ENE-WSW and N-S tectonic trends at different depths concordant with the surface.

A. INTRODUCTION

The area of study and its surroundings is built up of igneous and metamorphic rocks of late Precambrian age. The area is located in the Northern Eastern Desert of Egypt between latitudes 27° 48′ 30" N - 27° 49′ 30" N and longitudes 33° 4′ 25" E - 33° 5′ 35" E (Fig. 1). The relationship between breccia bodies and ore deposits is well documented in the literature (Phillips, 1972; Sawkins, 1984; Norman and Sawkins, 1985).

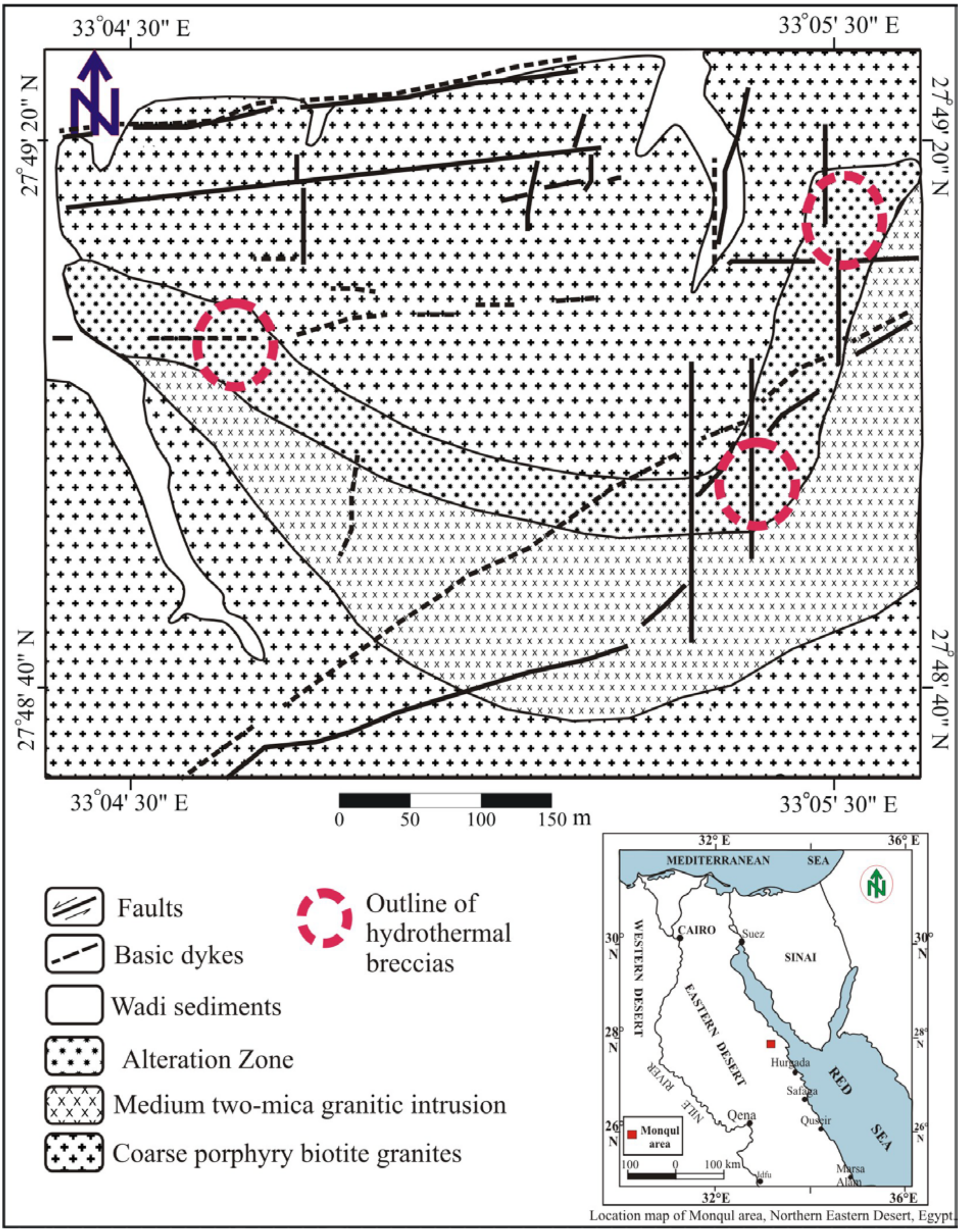

Fig. (1) Geologic map of South of Gabal Monqul, Northern Eastern Desert, Egypt .

Surface mapping of the area south of Gabal Monqul indicates different alteration types such as episyenitization and K-metasomatism. Advanced argillic alteration has been identified (Botros and Wetait, 1997). These alteration assemblages are typical of porphyry copper deposits (Gustafson, 1978, Sillitoe et al., 1990).

The aim of this study is to determine the geological and geophysical signature of the mineralized breccia in the studied area. The real advantage of using several geophysical methods in a coincident survey is the ability to screen the subsurface conditions at different depths using different ground geophysical parameters. This may allow for getting several consecutive depth images of the breccia bodies with depth, where the geophysical measurements are acquired. Magnetic survey was conducted to screen the detected mineralization at different depths. VLF-EM measurements were conducted to get a general overview of the subsurface distribution of mineralization in the study area. Gamma-ray spectrometry survey was a final step towards completing the image that explains the surface mode of occurrence of the detected mineralization. Gamma-ray spectrometry, based on chemical contrasts associated with shallow alteration halos, can be used as good criteria for uranium enrichment or depletion.

B. GEOLOGICAL SETTING

The Eastern Desert (ED) of Egypt is a part of the Arabian-Nubian Shield, which is constituted of arc(s)-inter-arc(s) rock associations that collided at a time span between 750-650 Ma (Stoeser & Camp, 1985; Kröoner et al., 1987; Abdel-Meguid, 1992). They are intruded by syn- to late-tectonic dioritic-granodioritic plutons at ~ 612 Ma as in Meatiq area (Sturchio et al., 1983). A flood of large ion lithophile (LIL) enriched granites with Dokhan volcanics flow were extruded and intruded the Shield (El Shazly et al., 1980).

The younger granites (YG) of south Gabal Monqul represent the youngest Pan-African intrusive rock unit. According to the field investigations, they can be divided into two granite types, showing variations in colour, grain size and mineral composition. The first type has a low relief, and consists of pale pink, coarse-grained biotite monzogranite with accessory minerals; apatite, titanite, opaque minerals, chlorite, epidot and sericite. This type has many subrounded to rounded xenoliths from mafic pebbles of different sizes. The second type has a moderate relief, and consists of pink, medium-grained equigranular two mica granitic intrusion, with accessory minerals; titanite, zircon, opaque minerals and chlorite.

The contacts between the two types are mostly sharp and well defined in the field. The second type has dyke-like bodies in some parts. The area is intersected by ENE-WSW and N-S faults. The breccia bodies are present between the two different granitic types mostly along the contact zone. These bodies are of circular shapes related to the faulting where extensive hydrothermal alteration events affected the host rocks along the contact between the granite types.

The granitic rocks of the studied area are cut by several basaltic, andesitic, doloritic and rhyolitic dykes, as well as pegmatites and quartz veins. The basic and acidic dykes are predominant, whereas intermediate dykes are relatively subordinate. All the dykes are relatively resistant to weathering, giving rise to pronounced ridges that cut across the country rocks. These dykes exhibit a marked variation in colour, texture, grain size and mineral composition. Some dykes show distinctive swelling and pinching in thickness; although the majority attains a uniform thickness. They are mostly vertical, vary in width from 0.3m to 15m, extending up to one kilometer in length. Sometimes, they form swarms running parallel to each other as in the western part of the study area. Three main trends: N-S, E-W and ENE-WSW to NE-SW were detected. The N-S and E-W dykes are basic in composition (andisitic to doleritic). The NE-SW trending dykes are mainly of rhyolitic composition and cross cut the E-W trending ones. The N-S trending dykes cut all the previous dykes (Fig. 1) so, they are considerable to the youngest in the study area.

C. CHARACTERISTICS OF THE MINERALIZED BRECCIA

1- General features

Three breccia bodies were recoded in the granite of south Gabal Monqul. Their outcrops are readily mappable, according to their pattern. The breccias are situated along the contact between coarse-grained and equigranular two mica granitic intrusion (Fig. 2). They have a circular to oval shape, with a diameter of about 50m to 70m.

The breccias are disaggregated with a highly variable fragment sizes ranging from 2cm to 50cm. The breccia fragments are typically angular while subrounded pieces are also present, secondary quartz are filling the inter-fragments.

The relatively simple features of the breccia are indicative of only one brecciation event. A well-developed oxidation zone with secondary iron and cupper oxides could be traced along fissures. Secondary minerals such as quartz are also observed in cavities. Cu mineralization is restricted mainly to the breccias and highest values are obtained in sheeting zones bordering the intensely-brecciated bodies at the intersection between ENE-WSW and NS fault trends.

2- Hydrothermal Alterations

In addition to the argillic alteration, other three main alteration assemblages are recognized in the examined area.

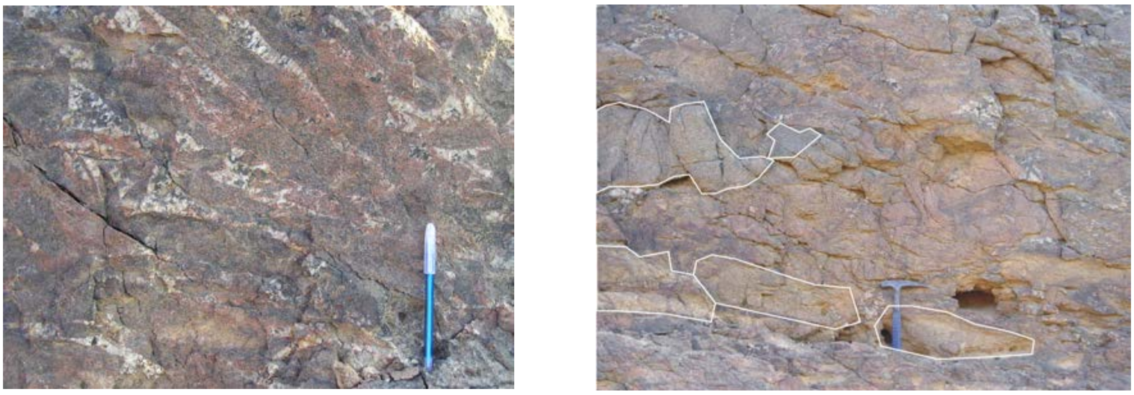

(a) (b)

Fig. 2: (a) Angular fragment and quartz interfragmental filling in breccia at the contact between the coarse-grained biotite and medium-grained grnaites. (b) Subangular to subrounded fragments of coarse-grained biotite grnaite in breccia.

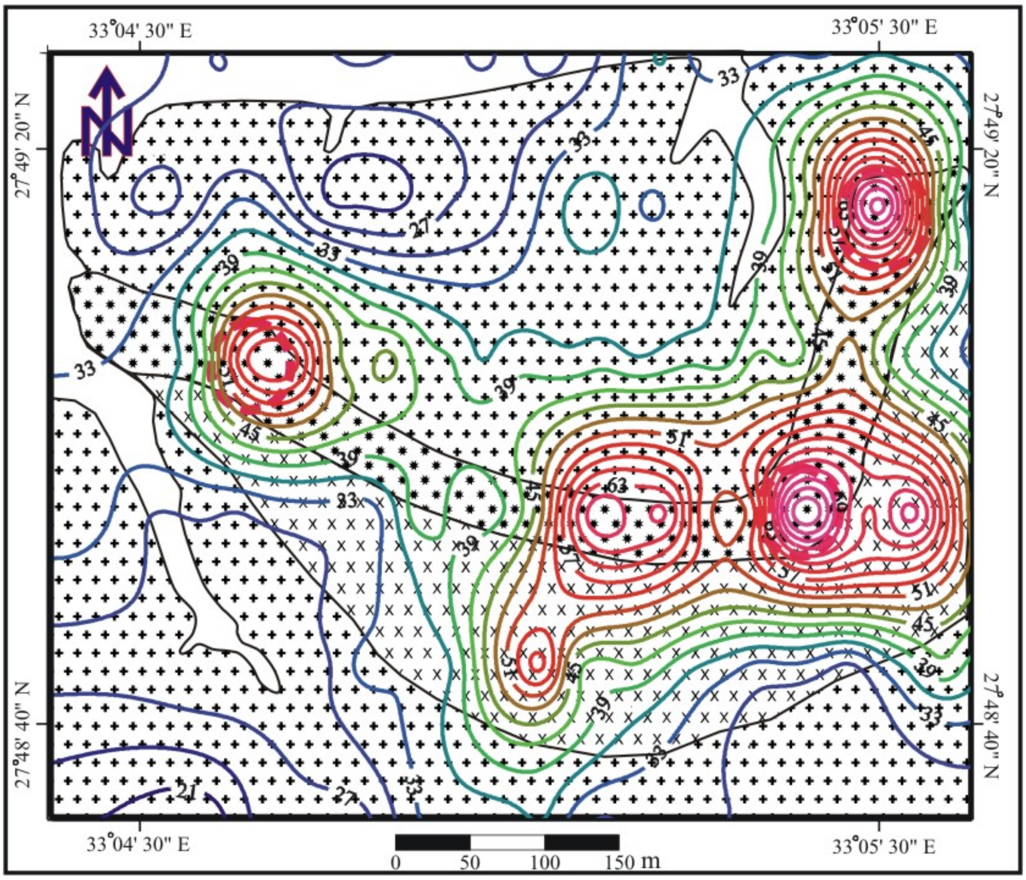

Fig. (3): Total count (T.C, Ur) radiometric contour map with the geology background of South of Gabal Monqul, Northern Eastern Desert, Egypt.

Episynitisation is the first alteration process where the quartz dissolution was followed by potassium metasomatism where the vugs of the dissoluted quartz were filled by K-feldspar. Hematitization are widely distributed especially around the breccia bodies. Specks of Au are linked to this alteration and are associated with enargite, bornite, covellite, chalcopyrite, chalcocite and altered magnetite (Botros and Watait, 1997). The barite veins of south Monqul are believed to be formed by the same fluids that were responsible for the advanced argillic alteration. Gold was noticed in different targets; as secondary quartz veinlets traversing granite porphyry, auriferous quartz veins that are distributed in the phyllic zone, and dispersed in barite veins associated with high sulphidation minerals.

D. GEOPHYSICAL FIELD PROCEDURE

a. GROUND γ-RAY SPECTROMETRIC SURVEY

Detailed ground geophysical measurements were carried out over the south Monqul granites using uniform square grid interval of 20m for the study area (600 m × 500 m). Ground gamma-ray spectrometric surveys have been conducted using a high-sensitive and well-calibrated gamma ray spectrometer (GS-256).

1- Total-Count (T.C., Ur) Radiometric Contour Map

South Monqul younger granites are discriminated as to have moderate to high radioactivity. However, the total-count radiometric map clearly exhibits distinctive anomalies over the mineralized breccia zone, reaching up to 80Ur. This is well demonstrated in the central parts of the study area in the form of separated high spots (Fig. 3). The T.C radioactivity ranges from 16 Ur to 40 Ur. They are encountered as large oval-shaped radioactive anomalies that divide it into two small semicircular anomalous zones. They are associated with the Cu- mineralization that lies to the east of the study area, representing the main central anomaly. The highest circular radioactive anomaly attain values >80 Ur and is located to the northeast of the study area.

2- Potassium (K %) Contour Map

Alteration zones can be readily detected from gamma ray spectrometric surveys that can identify K-rich alteration zones.

The potassium surface distribution contour map (Fig. 4) shows that the younger granite has a high level of K-content, ranging in intensity from 3 % to 6 %. This increase in K content results from the highly fractured and altered younger granites, beside the intrusions of late intrusiontic medium-grained granites, which are characterized by their relatively high radioactivities. The highly altered zone in the northeast of the study area attains values up to 8 K%. The central part of the area has a number of elongated anomalies reaching up to 6 %.

3- Equivalent Uranium (eU, ppm) Contour Map

The equivalent uranium content ranges from 4-12 ppmeU, is located over the younger granites (Fig. 5). It is controlled by main fault trends in the study area. The uranium distribution attains values up to 40 ppmeU over the mineralized breccias, where the Cu, Ba and Au-mineralization and prominent alteration features were detected. These anomalous zones are elongated mostly in the NW-SE and NE-SW directions, the highest one lies at the northeast of the mapped area along the NW-SE direction. They have circular to oval shapes, with diameters of about 70m.

4- Equivalent Thorium (eTh, ppm) Contour Map

The equivalent thorium (eTh) contour map (Fig. 6) shows that the concentration ranges from 16 to 24 ppmeTh on the younger granites. The zone, with eTh ranging from 28 ppm to 36 ppm, is encountered with different shapes trending in the E-W and N-S directions, and mostly coincides with the more differentiated medium equigranular two-mica granite which has dike-like bodies along those directions. Anomalies that possess eTh radioactivity more than 38 ppm are located as scattered spots in the altered zones.

5- eU/eTh Ratio Contour Map

The eU/eTh ratio ranges from 0.2 to 0.7 coincides with the mineralized breccias as semicircular anomalies. Three main anomalies are dissected by N-S faults and exhibit values reaching more than 5 (Fig. 7). There is a direct relation between uranium anomalies and eU/eTh ratio and this is a characteristic feature of the altered mineralized zone, where U-mobilization and enrichment is present. On the other hand, the unaltered younger granite, at the northern part of the study area, dos not have appreciated eU/eTh ratio or any distinctive anomalous signature and its contours take irregular shapes.

6-Uranium Mobility (eU-eTh/3.5) Contour Map

The construction of the uranium mobility map (Abdel Meguid et al., 2003) as eU versus eTh/3.5, enables delineating the limit between the negative contours (depleted zones) and positive contours (enriched zones). It is very helpful in defining the trends of uranium migration and delineating the most promising zones for uranium occurrence.

The (eU-eTh/3.5) mobilization map (Fig. 8) shows a good coincidence with high eU concentrations. The northern part of the study area, where unaltered younger granite exits have low level of radiations, mostly of negative values. The anomalies up to 30 ppm are found with dense contour lines superimposed on the mineralized zones in the NE-SW and NW-SE directions. This is essentially attributed to the uranium enrichment without any contribution from the adjacent granites. From the alternating negative and positive anomalies, the direction of uranium mobilization can be traced towards high positive anomalies.

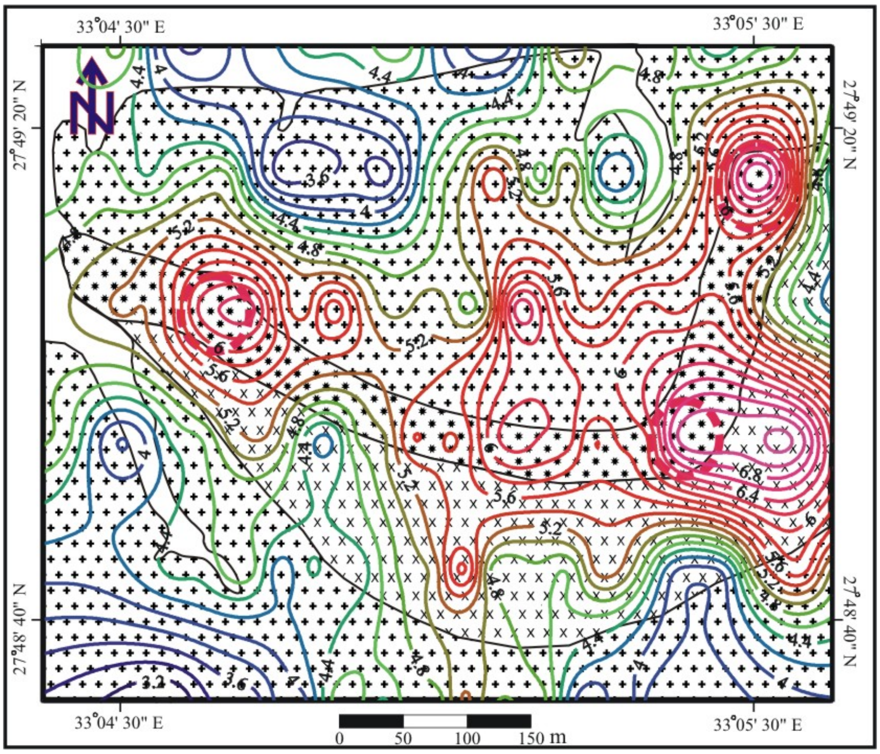

Fig. (4): Potassium (K, %) contour map with geology background of South of Gabal Monqul, Northern Eastern Desert, Egypt.

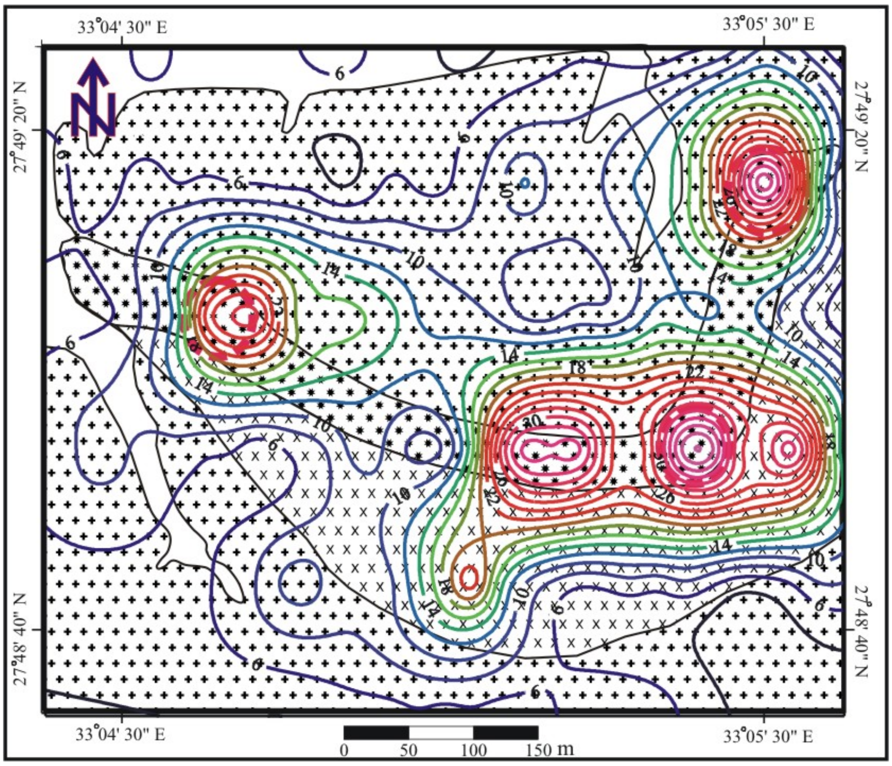

Fig. (5): Equivalent uranium (eU, ppm) contour map with geology background of South of Gabal Monqul, Northern Eastern Desert, Egypt.

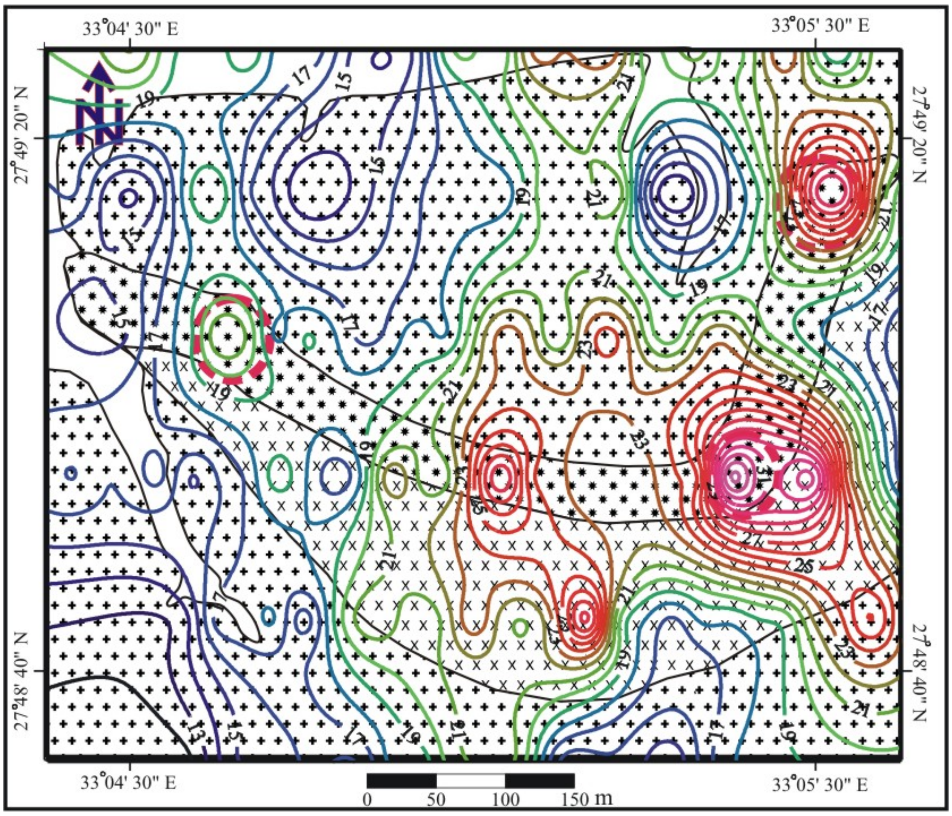

Fig. (6): Equivalent thorium (eTh ppm) contour map with the geology background of South of Gabal Monqul, Northern Eastern Desert, Egypt.

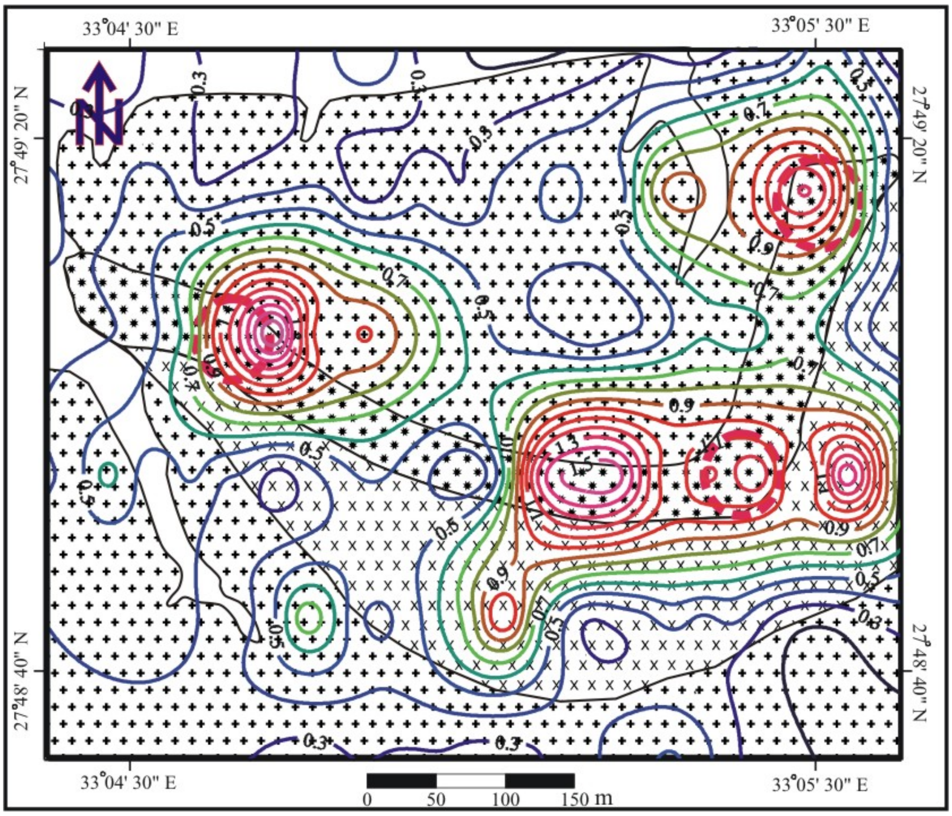

Fig. (7): eU/eTh ratio contour map with the geology background of South of Gabal Monqul, Northern Eastern Desert, Egypt.

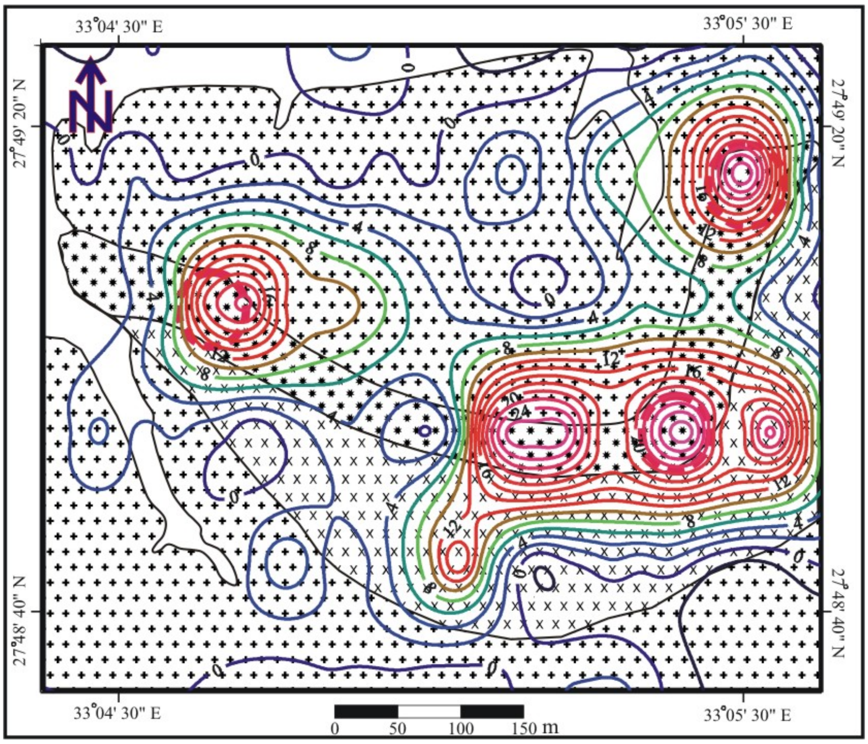

Fig. (8): Uranium mobility (eU-eTh/3.5) contour map with the geology background of South of Gabal Monqul, Northern Eastern Desert, Egypt.

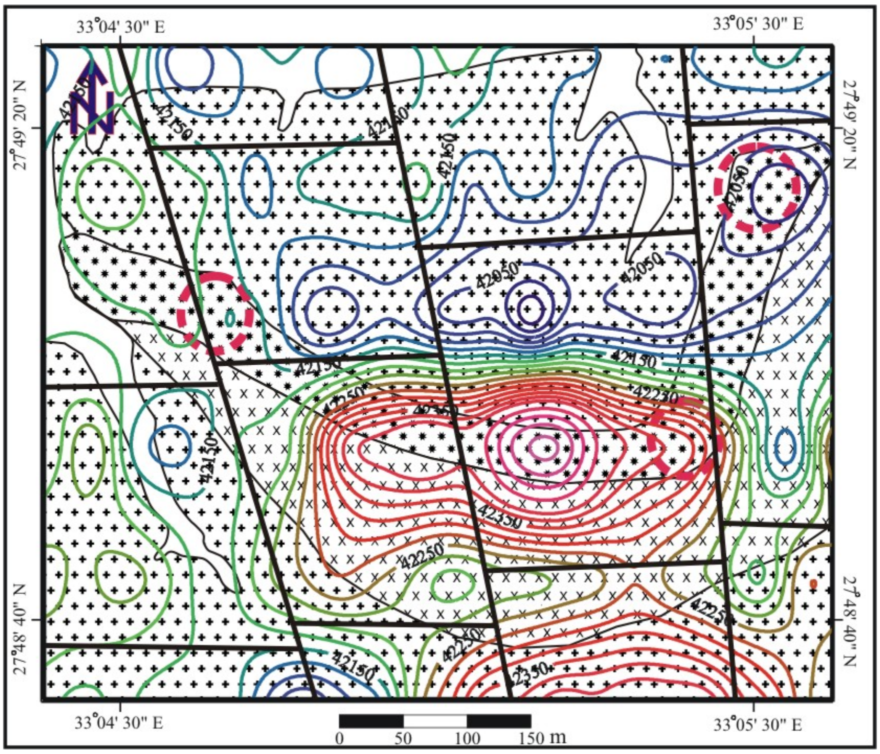

Fig. (9): Total magnetic intensity contour map (nT) with the main interpreted structures of South of Gabal Monqul, Northern Eastern Desert, Egypt.

b. GROUND MAGNETIC SURVEY

The exploration in south of Gabal Monqul area was directed to define the subsurface structural pattern for a uranium mineralization prospect, with strong contrasts in magnetic susceptibilities. Besides, the deep penetration sensitivity of the magnetic data provides direct exploration vectors for determining the continuity of any surfacial mineralization at depth.

Detailed ground magnetic measurements were carried out over the studied area using uniform square grid interval of (20×20 m). All the ground magnetic measurements were collected using the Scintrex proton magnetometer; model ENVI. The acquired survey data were displayed in the form of contour maps for the total intensity magnetic field and the filtered magnetic data.

1- Total Magnetic Intensity Contour Map

The total magnetic intensity map (Fig. 9) contains elongated positive and negative magnetic anomaly closures, associated with south Monqul mineralized zone. Most of the magnetic anomalies are distributed along two linear positive magnetic anomalies and one negative magnetic anomaly that trend approximately in an E-W direction. These anomalies are attributed more or less to the altered zone. The main magnetic anomaly possesses several positive peaks on the total-field magnetic map, but its amplitude, attaining about 42600 nT, is by far the largest of any of the recorded anomalies. The importance of these anomalies can be attributed to the strong contrast between the magnetic susceptibilities of the Monqul mineralization and the surrounding granites. The prominence of the sudden changes in spacing over an appreciable distance, that trend mostly in the N-S direction suggests discontinuity in depth, possibly due to effective of subsurface major faults.

2- Reduced to the pole for the total magnetic field Map (RTP)

The reduced to the pole magnetic field is used to determine automatically the source parameters as in the northern pole of the earth. The reduced to the pole contour map (Fig. 10) displays the South Monqul area with prominent linear belt of positive magnetic anomalies that extend across three main units, trending on E-W direction across the study area. The southern part of the study area is characterized by much broader positive magnetic anomaly elongated parallel to and coincides with the main mineralized zone. The formation of brecciated bodies is related to faulting where extensive hydrothermal alteration events affected the host rocks along the contact between the granite types.

The oval anomaly located at the central part of the study area is explained by the causative body coincides with a prominent elongated high magnetic anomaly. This agreement with the total magnetic intensity map (Fig. 9) suggests that the alteration has a large-extension buried body, extending along the E-W direction. The area is controlled by left-lateral strike slip faults trending nearly E-W, N-S and NW-SE, that dissect each other. In the southern part the N-S and NW faults are displace the E-W faults, whereas in the northern part the E-W faults displace the N-S faults.

3- Regional-Residual Separation

The isolation of magnetic anomalies was carried out for the total magnetic intensity map (Fig. 9) depending on the results of the energy spectrum analysis, using the Geosoft Program Package (Fig. 11). The method was applied to the total magnetic intensity data to obtain the average depth to the responsible subsurface geological sources as well as the differential magnetic response of each source ensemble that lie at a certain depth. This operation resulted in the construction of two maps namely; the regional magnetic-component anomaly map that is reduced to the magnetic pole (Fig. 12) at a depth of interface reaching 125 m and the residual magnetic-component anomaly map that is reduced to the magnetic pole (Fig. 13) at a depth interface reaching 26 m.

4- Regional Magnetic Anomaly Map

The South Monqul area is associated with distinct regional magnetic anomalies that are, elongated in the N-S direction, with amplitude reaching about 42800 nT (Fig.12). This anomaly is superposed on a much broader, roughly oval-shaped magnetic high that extends along the eastern part of the studied area. The western part of the area is characterized by very low magnetic anomaly (41700 nT) trending NNW-SSE. These two major anomalies are displaced with WNW-ESE faults. High potential hydrothermal mineralized fluids are proposed for the formation of breccias bodies through the intersection of the main tectonic trends in the area.

5- Residual Magnetic Anomaly Map

Narrow zones of positive and negative anomalies elongated mainly in the N-S and NNE-SSW directions embrace the surface projections of the South Monqul area (Fig.13). The central part is uplifted due to the effect of two normal faults that are accompanied by mineral solutions. The effect of tectonics and solutions may have resulted in the formation of the brecciated bodies.

6- Analytical Signal Magnetic Map

The analytical signal of the magnetic field is used to determine automatically the source parameters of dike-like structures. The analytical signal contour map (Fig. 14) displays the prominent linear belt of positive magnetic anomalies trending in the E-W direction across the study area. The central part of the study area is characterized by much broader positive magnetic anomaly. This anomaly is related to very high magnetic level in the RTP magnetic map that is is associated with the highly altered brecciaed body.

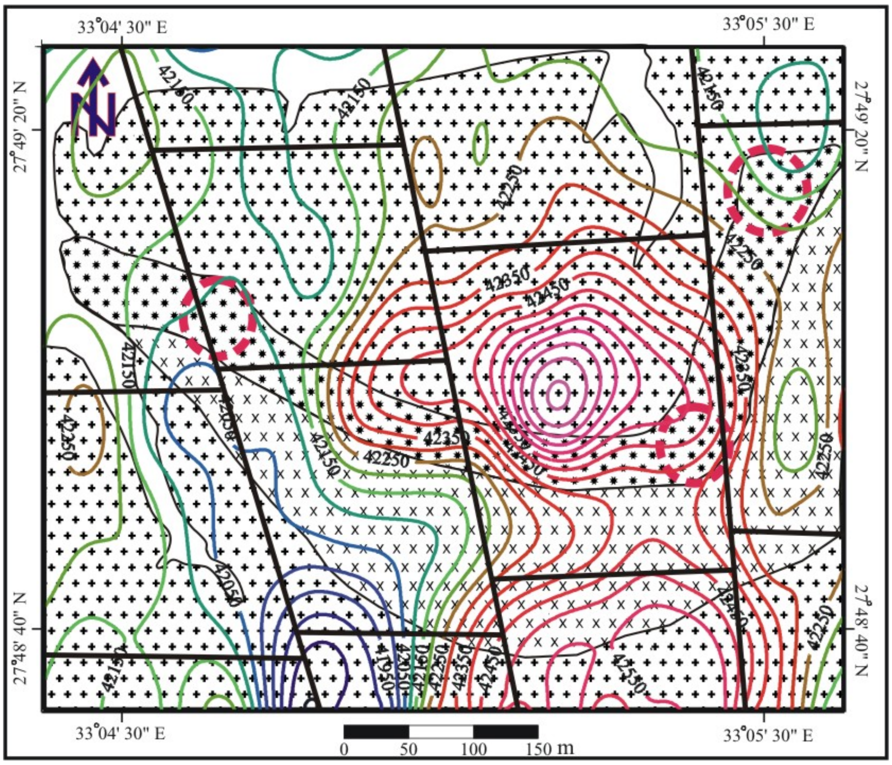

Fig. (10): Reduced to the pole magnetic contour map with the main interpreted structures of South of Gabal Monqul, Northern Eastern Desert, Egypt.

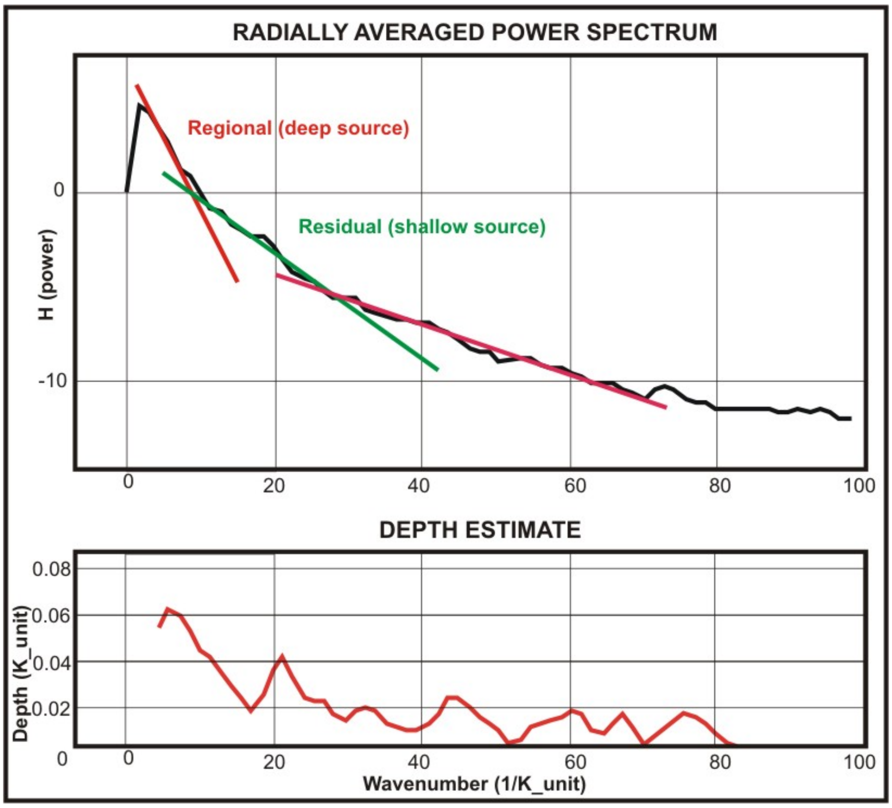

Fig. (11): Power spectrum of the total magnetic intensity data for regional-residual anomalies separation of South of Gabal Monqul, Northern Eastern Desert, Egypt.

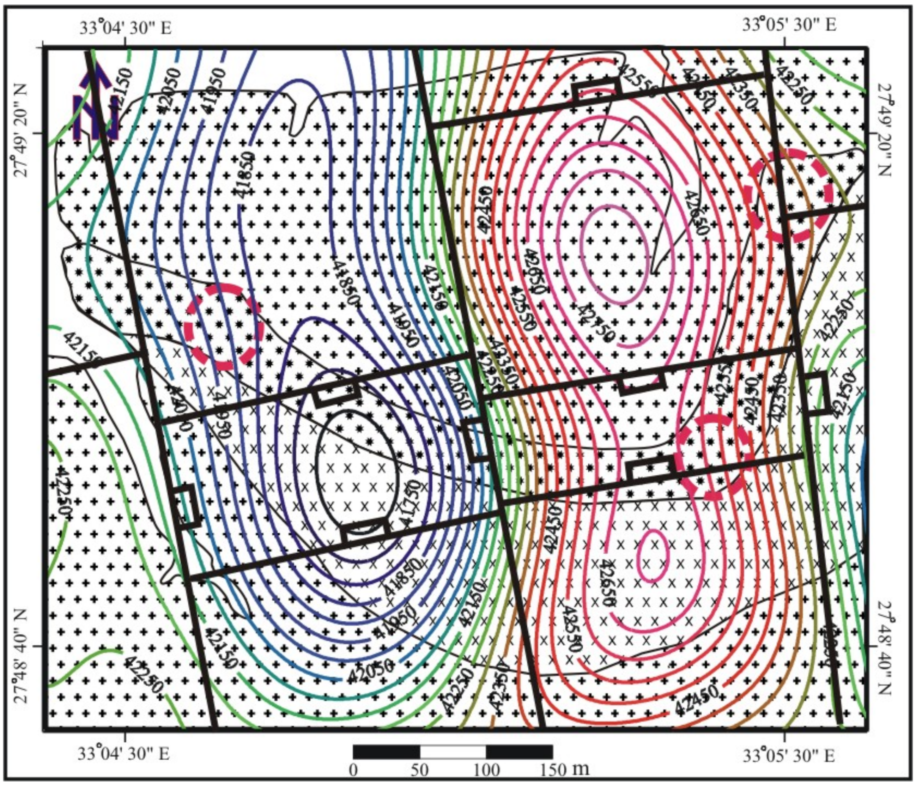

Fig. (12): Regional magnetic anomaly contour map with the main interpreted structures of South of Gabal Monqul, Northern Eastern Desert, Egypt.

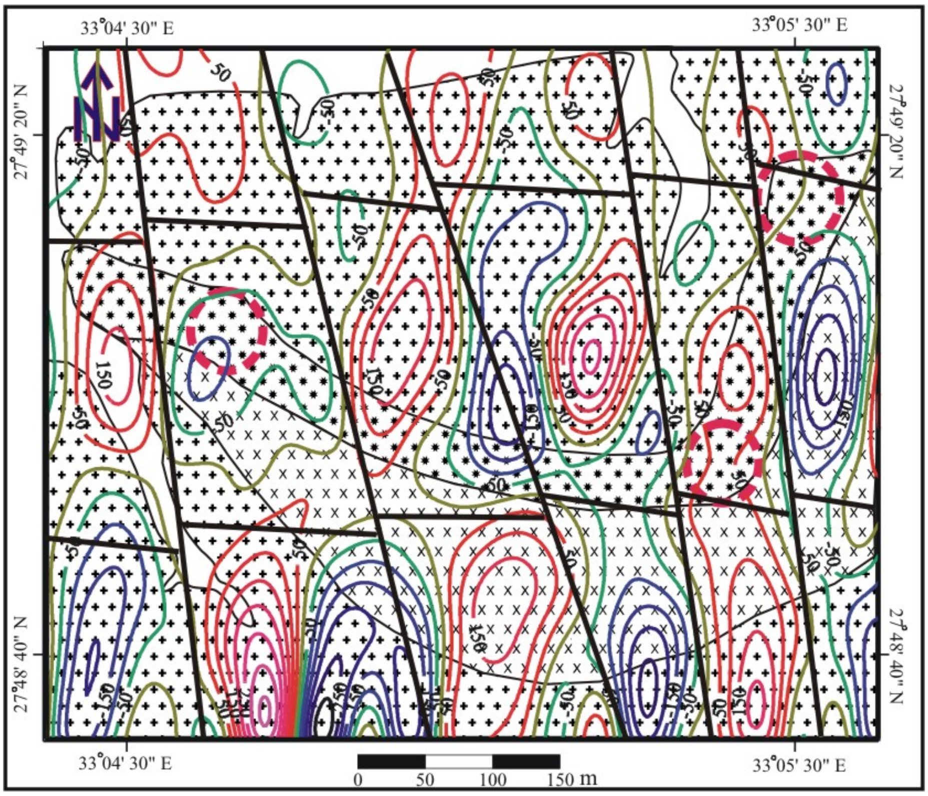

Fig. (13): Residual magnetic anomaly contour map with the main interpreted structures of South of Gabal Monqul, Northern Eastern Desert, Egypt.

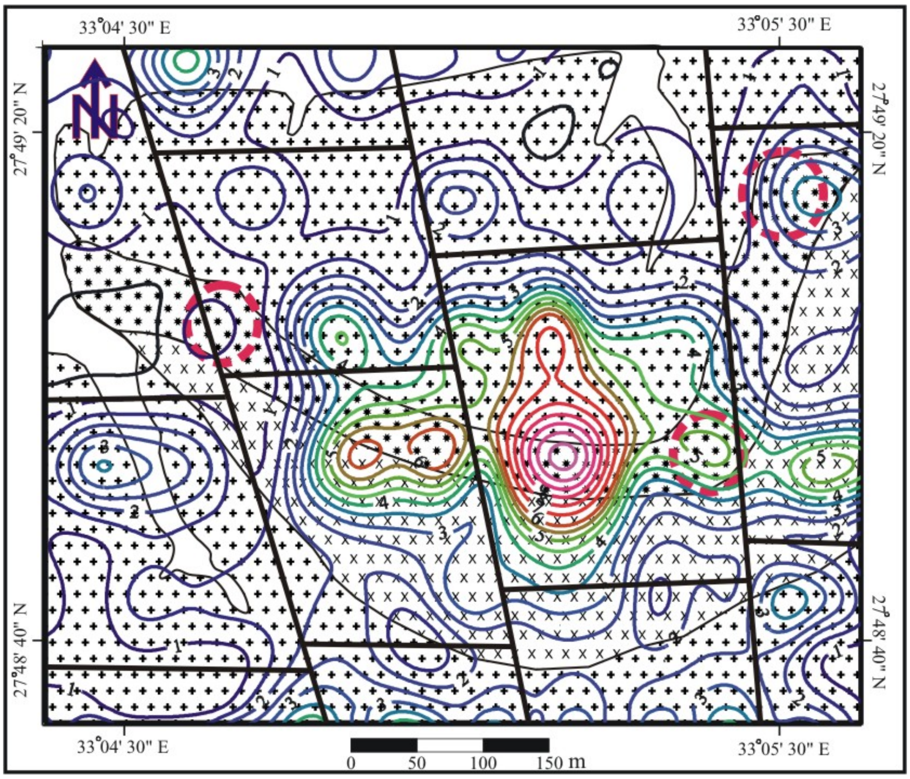

Fig. (14): Analytic Signal magnetic anomaly contour map with the main interpreted structures of South of Gabal Monqul, Northern Eastern Desert, Egypt.

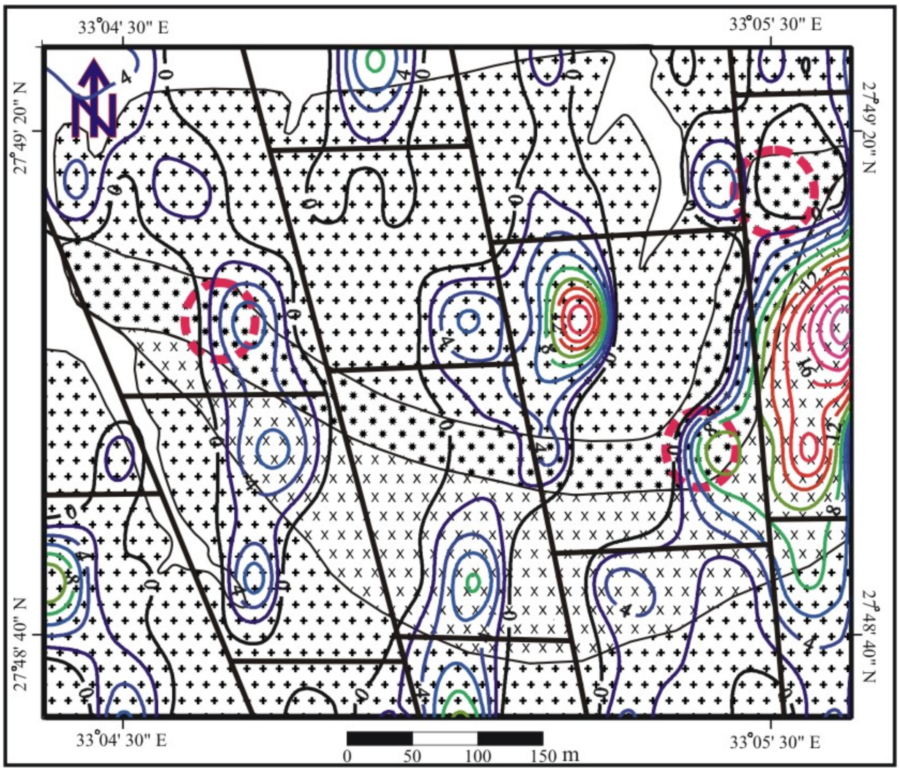

Fig. (15): VLF-EM (F=17.4 kHz) Fraser Filtered contour map with the main interpreted structures of South of Gabal Monqul, Northern Eastern Desert, Egypt.

This suggests that hydrothermal solutions were enriched with iron oxides and the high thickness of altered brecciaed body located at the center of the studied zone.

The interpreted structure played a considerable role in the enhancement of the deep and near-surface faulting systems affecting the study area. The interpreted structural map deduced from the analytic magnetic data shows mainly two intersecting sets of E-W and NW-SE trending faults. The first interpreted group of faults comprises those with nearly E-W trend. These faults represent the main trend through which hydrothermal solutions were flown causing the mineralization. These faults of deep-source regional contacts are dissected and displaced by the NW trending faults. Most of these faults cause sudden change in the contour spacing over an appreciable distance which suggests a discontinuity in depth due to these normal dip slip faults.

c. GROUND VLF-EM SURVEY

1- Filtering and Interpretation of VLF-EM Data

The point where the tilt angle crosses over from being positive to negative polarity is usually interpreted as being immediately above the top of the conductor causing the anomaly. Fraser (1969) designed a filter to shift the tilt angle data by 90 degrees, so that the crossover and inflection points become peaks. The Fraser filter uses four consecutive data points, where the data were acquired at a regular interval and can be applied very simply using a spread sheet. The sum of the first and second data points is subtracted from the sum of the third and fourth values and plotted at the midpoint between the second and third tilt angle stations. These yield either negative or low positive values. The values are plotted on the lines as the filter passes, and the positive values contoured to produce a map. The interpretation of filter plots is qualitative. Very sharp responses indicate shallow sources and conversely, broader anomalies indicate progressively deeper sources. The contouring connects responses from line to line and serves to delineate the trends of conductive zones.

2- Fraser Filtered VLF-EM Map

The VLF-EM Fraser filtered contour map (Fig. 15) using frequency (F=17.1 kHz) of the study area shows that the hydrothermal breccias are located along gradational values of conductivity that are outlined by the contour lines from 0 to 10. The graditional values of conductivity is due to the degree of brecciation and the mount of quartz interfragmental filling which plays an important role in fluid circulation and uranium redistribution. There are strong conductivity anomalies with great amplitudes, more than breccias up to contour line 22, demonstrated particularly well in the eastern part of the study area, where the faulted alteration zones possessing high conductivities predominate.

Meanwhile, the granites are characterized by relatively weak conductive zones that generally follow the N-S trending normal faults. The separated parts of positive anomalies are associated with the mineralized faulted zones. The negative anomalies to the east of the study area are due to high resistive materials. Consequently, close correlations are observed between the positive VLF-EM anomalies and the existing mineralization. Meanwhile, the pronounced negative VLF-EM anomalies are noticed in the granites. The magnetic and apparent conductivity maps clearly exhibit distinctive anomalies, particularly in central regions of the area, where the mineralization is associated with high magnetic susceptibilities and gradational electric conductivities. An excellent correlation is observed between the conductivity map and the residual magnetic map of the area that provide a means of distinguishing between the overburden and the subsurface conductivity responses.

SUMMARY AND CONCLUSIONS

Three breccia bodies are recorded in the granites of south Gabal Monqul. These breccias are situated along the contact zone between the coarse-grained biotite granite and medium two mica granites. They have a circular to oval shape, with a diameter from 50m to 70m. The breccia fragments are typically angular, while subrounded pieces are present. A well-developed oxidation zone with secondary iron and copper oxides along fractures and growth of secondary quartz in cavities is present. An extensive hydrothermal alteration event affected the host rocks where Cu, Ba and Au were deposited in bordering zones of intensely-brecciation. All these features are controlled by two master tectonic trends, nearly E-W intersected by N-S system faults. The hydrothermal origin is proposed for the breccia and mineralizations.

The γ-ray spectrometric maps of South Monqul granites show that the mineralized zone is clearly detected from the sharp increase in the eU values and their ratio with eTh as well as from the marked increase of the K values. The direct increase of eU/eTh ratio with eU and inverse relation with eTh in these breccia bodies is attributed to post-intrusiontic redistribution of uranium in contrast to thorium. The processes of uranium mobilization towards the alteration haloes are very important as such altered rocks were subjected to mineral-bearing solutions.

The reduced to pole magnetic intensity map of South Gabal Monqul shows many circular, elongated and oval-shaped positive and negative magnetic anomalies, associated with South Monqul mineralized breccias. The low magnetic values on various magnetic maps for the younger granites reflect the low magnetic susceptibilities of these rocks. South Monqul is associated with conspicuous, elongated positive conductivity anomalies. Conductivity is essentially due to the mineralization, with no contribution from the adjacent granites. These wide VLF-EM anomalies are typical of good conductors.

Integrating the results of the different three geophysical methods used to survey the study area led to state that the subsurface mineralized zone in the study area is formed by hydrothermal fluids. These fluids were ascending slowly by the high resistance of the granitic rocks, creating a heap of copper mineral concentrations in the deeper part underneath the central parts of the highly-altered area. However, some of these hydrothermal fluids found their path through the E-W fault plane creating the elongated shallower concentrations of copper mineralization. In a later stage, mineralized zones were displaced by the N-S fault system.

REFERENCES

Abdel-Meguid, A. A., 1992: Late Proterozoic Pan African tectonic evolution of the Egyptian part of the Arabian-Nubian Shield. M. E. R. C. Ain Shams Univ., Earth Sc. Ser., Vol. 6, pp. 13-28.

Abdel Meguid, A. A., Cuney M., Ibrahim, T. M., Ali Kh. G., and Gaafar I. M., 2003: New application of systematic gamma ray spectrometric measurements. Asiut, Egypt Vol. 1, pp. 873 - 878.

Baker, E. M., and Andrew, A. S., 1991: Geologic fluid inclusion, and stable isotopic studies of the gold-bearing breccia pipe at Kidston, Queensland, Australia Econ. Geol., Vol. 86, pp. 810- 830.

Botros, N. S., and Wetait, M. A., 1997: A possible porphyry copper mineralization in south Um Monqul, Eastern Desert, Egypt. Egypt J. Geol., Vol. 41, No. 1, pp. 175-196.

Dickson, B. L., and Scott, K.M., 1997: Interpretation of aerial gamma ray surveys - adding the geochemical factors. AGSO Journal of Australian Geology and Geophysics, Vol. 17, No. 2, pp. 187-200.

Elshazly, E. M., Dixon, T. H., Engel, A. E. J., Abdel Meguid, A. A. and Stern, R. J., 1980: Late Precambrian crustal evolution of Afro-Arabia from oceanic arc to craton. Egypt J. Geol., Vol. 24, No. 1- 2, pp. 101-121.

Fraser, D.C., (1969): Contouring of VLF-EM data. Geophysics, Vol. 34, pp. 958-967.

Franklin, J.M., 1996: Volcanic-associated massive sulphide base metals. In Geology of Canadian Mineral Deposit Types, (ed.) O.R. Eckstrand, W.D. Sinclair and R.I Thorpe; Geological Survey of Canada, Geology of Canada, pp. 158-183.

Gustafson, L. B. (1978): Some major factors of porphyry copper genesis. Economic Geology, Vol. 73, pp. 600-607.

Kröner, A, Greiling, R., Reischamann, T., Hussein, I. R. M., Stern, R. J., Durr, S., Kruger, I., and Zimmer, M. 1987: Pan African crustal evolution in the Nubian segment of northeast Africa . Series, Washington D. C., Vol. 17, pp. 235-257.

Norman, D. I., and Sawkins, F. J. , 1985: The Tribag breccia pipes: Precambrian Cu-Mo deposits, Batchawana Bay, Ontario, Canada. Econ. Geol., Vol. 80, pp. 1593-1621.

Phillips, W.J. (1972): Hydraulic fracturing and mineralisation. Journal of the Geological Society of London, Vol. 128, pp. 337-359.

Poulsen, K.H. and Hannington, M.D., 1996: Volcanic-associated massive sulphide gold. In Geology of Canadian Mineral Deposit Types, (ed.) O.R. Eckstrand, W.D. Sinclair and R.I Thorpe; Geological Survey of Canada, Geology of Canada, pp. 183-196.

Sawkins, F. J., 1984: Metal deposits in relation to plate tectonics. Springer, Berlin, 325 p.

Shives, R.B.K., Charbonneau, B.W., and Ford, K.L., 1997: The detection of potassic alteration by gamma-ray spectrometry – Recognition of alteration related to mineralization. *In* Proceedings of Exploration, 97: Fourth Decennial International Conference on Mineral Exploration, *Edited by*A.G. Gubins, pp. 741-752

Sillitoe, R. H., Angles, C. A., Comia, G. M., Antioguia, E. C. And Abeys, R. B. 1990): An acid-sulphate type lode gold deposit at Nalesbitan, Luzon, Philippines. In: Epithermal gold mineralization of the circum-Pacific: Geology, geochemistry, Origin and exploration. (Edited by Hedenquist, J. W., White, N. C. and Siddeley, G.) Journal Geochemical Exploration Vol. 35, pp. 1575-1591.

Stoeser, D. B., and Camp, V. E., 1985: Pan-African micro plate accretion of the Arabian Shield. Geol. Soc. Am. Bull., Vol. 96, pp. 817-826.

Sturchio, N., Sultan, M., Sylvester, P., Batiza, R., Hedge, C., and Abdel-Meguid, A. A., 1983: Geology, age and origin of Meatiq Dome: Implications for the Precambrian stratigraphy and tectonic evolution of the Eastern Desert of Egypt. Jeddah, Saudi Arabia, King Abdul Aziz Univ., Fac. Sc. Bull., Vol. 6., pp. 127-143.